Interannual Variability in the Gulf of Alaska during the 1991–94 El Niño

MARIA FLATAU AND LYNNE TALLEY

Scripps Institution of Oceanography, University of California, San Diego, La Jolla, California

DAVID MUSGRAVE

University of Alaska at Fairbanks, Fairbanks, Alaska

(Manuscript received 7 May 1998, in final form 1 July 1999)

ABSTRACT

Mass and heat budgets in the Gulf of Alaska during the 1991–94 El Niño are examined using hydrographic data from several cruises undertaken as part of the International North Pacific Ocean Climate program and the repeated Canadian hydrographic sections out to Ocean Weather Station Papa. The geostrophic ocean circulation resulted in convergence of heat into the region in spring 1992 and spring 1993. The advective heat convergence in spring 1992 corresponded to an average surface heat flux from the ocean to the atmosphere of about 74 W m^{-2} in comparison with only 30 W m^{-2} during spring 1993. The larger ocean heat loss to the atmosphere in 1992 followed a winter of large tropical SST anomalies and anomalously low pressure in the Aleutian low.

1. Introduction

The importance of the tropical SST pattern for midlatitude extratropical atmospheric circulations has been recognized for a long time. Tropical circulation anomalies forced by tropical SST anomalies propagate poleward and influence the weather in midlatitudes, forming a well-defined teleconnection pattern (Horel and Wallace 1981). In the northern Pacific, the major teleconnection pattern, called the PNA (Pacific–North American), associates positive SST anomalies in eastern Pacific with strengthening of the Aleutian low and midlatitude westerlies, and southeastward displacement of the Pacific storm tracks (Trenberth and Hurrel 1994; Hoerling and Ting 1994). Increased wind speeds and southward advection of cold arctic air enhance surface latent and sensible heat fluxes, causing cold SSTs and a deeper mixed layer in the central and western Pacific, while advection of warm and moist air in the east reduces the heat oceanic heat loss along the North American coast (Alexander 1992).

The Tropics can influence the subarctic heat storage and SST anomalies in two ways: quickly through the ''atmospheric bridge'' between the Tropics and midlatitudes (Lau and Nath 1996) and varying air–sea fluxes, and slowly through ocean processes such as propagating coastal Kelvin waves (White 1994; Meyers et al. 1996; Lagerloef 1995). During periods of excess warmth in the Tropics (El Niños), the atmospheric teleconnection produces strengthened westerlies in the midlatitude North Pacific. The resulting SST anomaly pattern is cold in the central and western subpolar gyre where the strong winds create anomalous cooling and also where the cold, southward-flowing western boundary current might advect more cold water into the gyre. In the eastern subpolar region, a strengthened subpolar gyre advects anomalously warm water northward along the eastern boundary into the Gulf of Alaska. The zero crossing between colder and warmer SST associated with ENSO is located in the Gulf of Alaska.

The entire Pacific is also subject to decadal-scale variations with a spatial pattern of variability similar to that of ENSO but with nearly equal amplitude in the Tropics and subtropical–subpolar regions (Zhang et al. 1997).

Midlatitude ocean temperature anomalies can, in turn, influence midlatitude atmospheric circulation (Latif and Barnett 1994) or propagate equatorward and affect the variability in the Tropics (e.g., Zhang et al. 1997). Midlatitude ocean–atmosphere interaction could be particularly important for long timescale variability of the atmosphere–ocean system. Various feedback mechanisms are presently being investigated in numerical studies that try to assess the role of midlatitude SST and climate variability (Latif 1998).

In this paper we examine the circulation and heat budgets in the Gulf of Alaska during the 1991–94 El Niño, using data from hydrographic cruises conducted

Corresponding author address: Dr. Maria Flatau, Scripps Institution of Oceanography, University of California, San Diego, Physical Oceanography Research Division, La Jolla, CA 92093-0221.
E-mail: mflatau@ucsd.edu

in fall 1991, spring 1992, fall 1992, and spring 1993. This permits us to see if variations in the heat budget were consistent with variations in climate indices. The heat budget calculated using an extended dataset, including seasonal heat storage information, also permits us to comment on the recent findings of Moisan and Niiler (1998) of net surface heat gain by the ocean from the atmosphere in the Gulf of Alaska. The hydrographic cruises were carried out as part of a joint Russian–Canadian–U.S. program called the International North Pacific Ocean Climate (INPOC) program. In addition, the repeated Canadian hydrographic sections from Vancouver Island to ocean weather station Papa were used to complete a box around the Gulf of Alaska for the purpose of heat budgets. The datasets are described more fully in section 3.

The 1991–94 El Niño was rather unusual. As shown by Trenberth and Hoar (1996), statistical analysis indicates that it was unexpected given the previous record and may have been partly caused by anthropogenic changes. During this event, persistent warm SST anomalies were observed in the central equatorial Pacific from 1990 to June 1995, while a series of warm events developed in the eastern Pacific in 1991–92, 1993, and 1994 (Goddard and Graham 1997; Trenberth and Hoar 1996).

The first INPOC cruise (fall 1991) took place during increasing warm anomalies in the eastern equatorial Pacific that reached their peak in the winter of 1991/92. SST anomalies in the Tropics receded for a few months at the end of 1992, suggesting a return to normal conditions, but positive SST anomalies in the Tropics returned in early 1993. This development allows us to compare the circulation in the North Pacific during the period with large SST anomalies in the Tropics (followed by our spring 1992 dataset) versus more ''normal'' conditions (represented by our spring 1993 dataset).

In addition to hydrographic measurements from INPOC, National Centers for Environmental Prediction (NCEP)–National Center for Atmospheric Research (NCAR) reanalysis data were used to evaluate atmospheric surface fluxes. The NCEP–NCAR project data uses a state-of-the-art assimilation system and database, enhanced with as many observational sources as possible (Kalnay et al. 1996). It provides the best available estimate of the total surface flux. Heat storage in the Gulf of Alaska was estimated using gridded heat storage data from the Joint Environmental Data Analysis Center (JEDA) project (White 1995). The monthly SST anomalies used in this paper are the product of the Integrated Global Ocean Services System. These SST anomalies are calculated from weekly SST data and include ship-, buoy-, and bias-corrected satellite data (Reynolds 1988).

2. North Pacific atmospheric response to 1991–94 El Niño

In 1991–93, the SSTs in the Tropics were dominated by an unusually long, warm ENSO event. The SST anomalies and Southern Oscillation index (SOI) varied, but the SSTs did not return to normal conditions, and the SOI remained negative from 1991 until early 1995. The event was particularly strong in the winter of 1991/92, weakened in late 1992, but returned by the beginning of 1993.

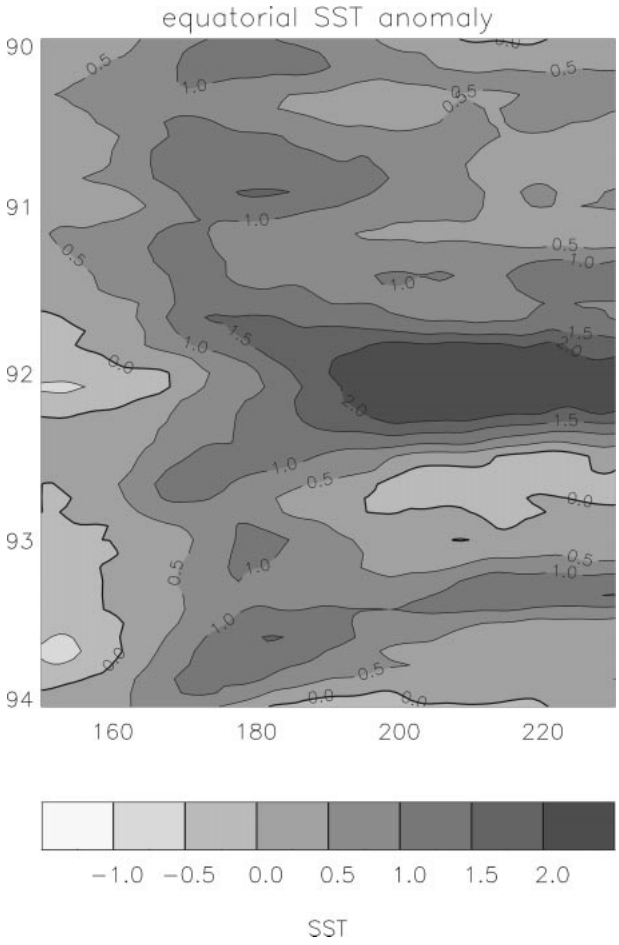

FIG. 1. 1990–94 equatorial SST anomalies [from National Meteorological Center (now NCEP) blended SST data].

During 1990 and early 1991 the development of a weak El Niño was indicated by warm SST anomalies in the central equatorial Pacific (Fig. 1) and a slightly negative SOI (McPhaden 1993). Warm anomalies appeared in the eastern equatorial Pacific in mid-1991 and rapidly strengthened in September 1991. This eastward progression of the SST anomalies was a consequence of the strong westerly wind burst that developed west of the date line at the equator in August–September (McPhaden 1993). Major westerly bursts in November–December 1991 and January 1992 advected warm anomalies farther east, with the maximum anomalies about 2°C at 155°W. The lowest values of the SOI were reached in January and March 1992. The warm tropical SSTs retreated in March–April 1992. In April 1992 the SOI began to rise, and it became positive in August

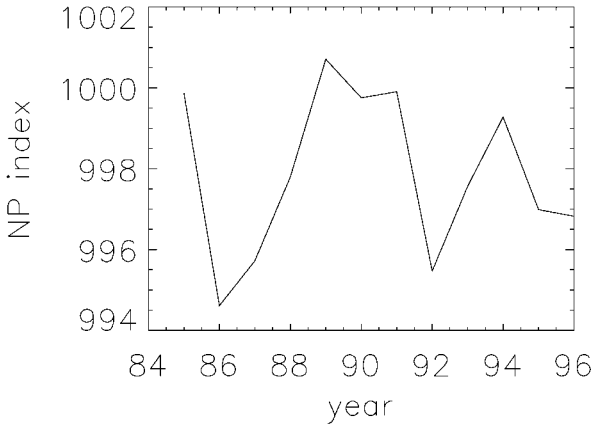

FIG. 2. The NP index defined as weighted sea level pressure over the region 30°–65°N, 160°E–140°W from Nov to Mar, from 1985 to 1996. Pressure data are from NCEP–NCAR reanalysis.

1992. However, in late 1992, the westerly wind anomalies in the western and central Pacific intensified, and El Niño conditions returned by spring 1993.

In response to increased warm anomalies in the tropical Pacific, the Aleutian low deepened rapidly in late 1991 (Fig. 2), as quantified by the North Pacific (NP) index, defined by Trenberth and Hurrel (1994) to describe the PNA teleconnection pattern. Following Trenberth and Hurrel (1994) the NP index is calculated here as the area-weighted sea level pressure over the region 30°–65°N, 160°E–140°W from November to March.

After a period of relatively high values in the late 1980s, corresponding to the 1989 La Niña (Fig. 3a), the North Pacific surface pressure dropped in the winter of 1991/92 (Fig. 3b). This pressure drop in the North Pacific corresponded to SST and convection anomalies developing over the eastern equatorial Pacific in late 1991. In the winter of 1991/92, the low pressure system centered over the Gulf of Alaska created strong southwesterly flow over the eastern North Pacific and the Gulf of Alaska and strong westerlies over the central North Pacific. In the following winter, El Niño in the Tropics weakened and convective activity receded toward the west. In response, the Aleutian low moved west and weakened. Midlatitude westerlies over the western North Pacific remained fairly strong, but the southwesterly flow over the eastern portion of the basin weakened substantially.

Temporary recession of El Niño in late 1992 was accompanied by a change in surface fluxes in the North Pacific (Fig. 4). The surface flux pattern in 1991/92 corresponded to the ''canonical'' El Niño pattern, while the 1992/93 change in the circulation brought a return to more normal conditions in the North Pacific. In winter 1991/92, the increased cyclonic circulation was associated with an inflow of the warm, moist air from the south and caused increased precipitation in the eastern North Pacific, especially along the North American shore. The presence of the warm moist air also reduced the latent and sensible heat fluxes in the eastern North Pacific, while the sensible and latent heat loss in the central and western Pacific increased as a result of stronger circulation and advection of dry and cold Arctic air. The change in NCEP–NCAR reanalysis radiation fluxes was consistent with outgoing longwave radiation patterns, with shortwave flux reduction in areas of increased cloudiness—that is, along the North American coast and between 25° and 35°N—while in the central North Pacific, the shortwave flux was larger in the El Niño winter 1991/92. Since the radiative short- and longwave flux anomalies opposed each other and were smaller than latent and sensible heat fluxes, the total flux pattern was mostly determined by evaporation and sensible heat fluxes.

3. Variability of mass and heat fluxes in the Gulf of Alaska

In this paper we concentrate on the circulation and heat budget in the Alaskan gyre, which is the eastern portion of the cyclonic subpolar gyre. The Alaskan gyre is bounded on the east by the northward-flowing Alaska Current that converges into the strong, westward-flowing Alaskan Stream just upstream of Kodiak Island. Part of the Alaskan Stream flows northward through the Aleutian Islands into the Bering Sea, and part continues westward where it joins the Bering Sea outflow in the East Kamchatka Current. The Alaskan gyre is bounded to the west at about the date line, where the Aleutian Islands are at their southernmost point. The cyclonic circulation west of this is referred to as the western subarctic gyre.

It has been generally thought that the Alaskan gyre is a region of net heat loss from the ocean to the atmosphere since warm water is advected northward in the east and colder water is advected westward in the Alaskan Stream. The total amount of heat gain/loss in the Alaskan gyre is small, on the order of about 20 W m^{-2} (e.g., Talley 1984), which is close to the measurement error using bulk formulas. Moisan and Niiler (1998) recently examined the surface heat fluxes in the North Pacific. They chose preferred bulk formulations for air–sea fluxes based on heat storage information derived from surface drifter temperatures and XBT profile data. Their surprising conclusion is that the Alaskan gyre actually gains heat from the atmosphere, also at a rate of about 20 W m^{-2}.

We use 2 yr of hydrographic data to examine the heat budget in the Gulf of Alaska and its variability under changing atmospheric forcing. From fall 1991 to spring 1993, four INPOC cruises were conducted in the subpolar and subtropical North Pacific (Fig. 5). The spring 1992 INPOC cruise was a joint effort between the Institute of Ocean Sciences (IOS) in Sidney, British Columbia, Canada; and the Far Eastern Regional Hydrometeorological Institute (FERHI) and the Pacific Oceanological Institute (POI) Far Eastern Branch of the Acad-

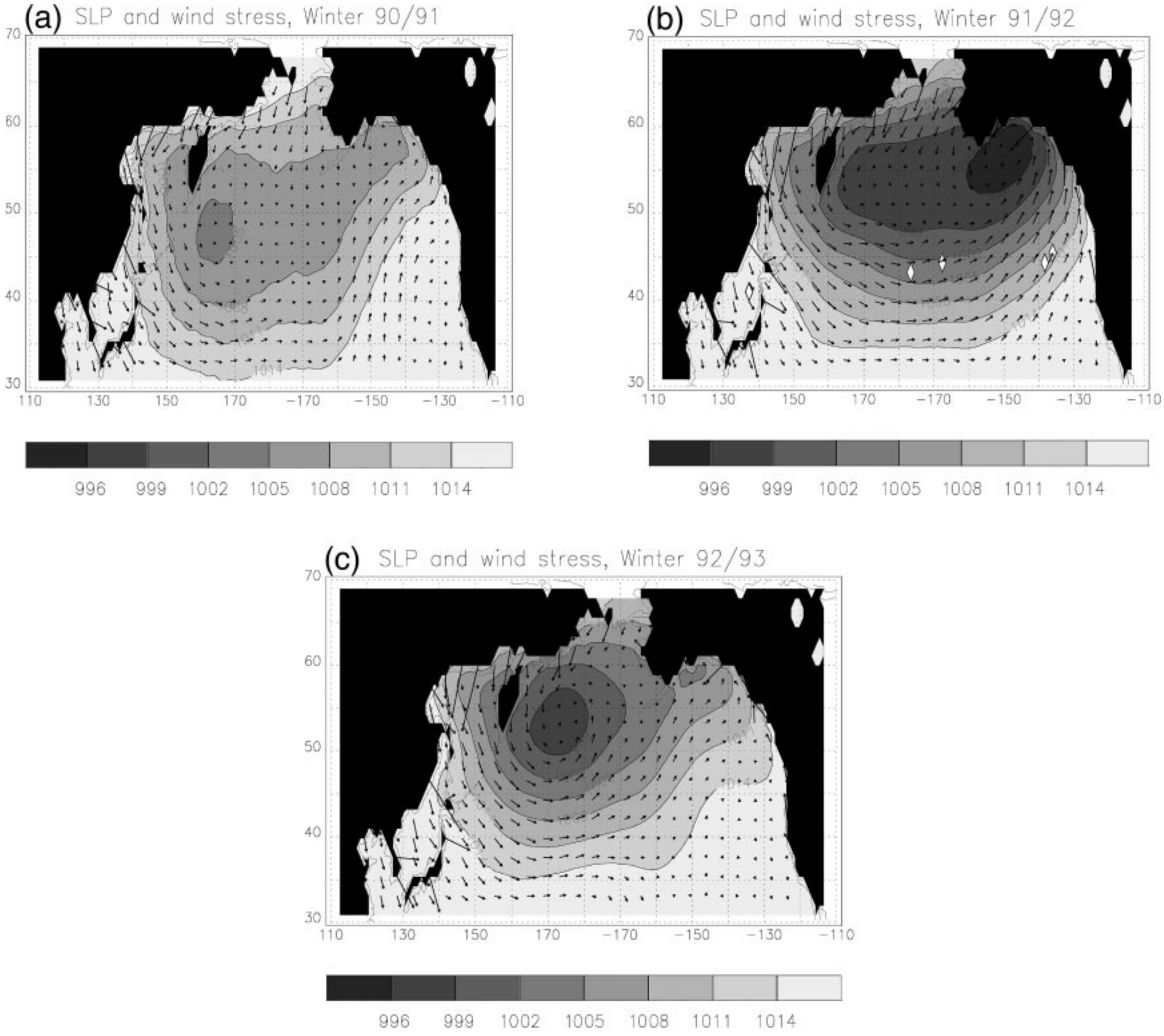

FIG. 3. Sea level pressure and wind stress in the North Pacific (data from European Centre for Medium-Range Weather Forecasts analysis) averaged over winter months (Nov–Feb): (a) winter of 1990/91, (b) winter of 1991/92, and (c) winter of 1992/93.

emy of Sciences, both in Vladivostok, Russia. The spring 1993 cruise added participation by Scripps Institution of Oceanography and the University of Alaska. All cruises were carried out on the *Priliv*, a FERHI research vessel. Chief scientists were O. Pyatin (FERHI), G. Yurasov (POI), and N. Vannin (POI).

For our Gulf of Alaska calculations, we use the INPOC ''box'' bounded on the north and east by the North American shore and on the west and south by the 50°N and 160°W INPOC transects (Fig. 5). Measurements from the Canadian ''Line-P'' cruises (Tabata 1991) supplement the INPOC data in the eastern portion of the 50°N transect in Fig. 5.

Ocean temperature and salinity were measured on all cruises using a Guildline CTD (conductivity–temperature–depth) from the surface down to approximately 1500 dbar. The Line-P stations from spring 1993 extend to 2000–3000 dbar. The CTD data were processed from time series to 1-dbar vertical spacing using IOS's standard procedures for Guildline CTD data. The spring 1993 dataset also included discrete rosette sampling for salinity and oxygen, permitting more careful calibration of the CTD data. For the purposes of this paper, the increased accuracy was not required, and so all datasets can be used together.

From these measurements, geostrophic mass and heat transports were calculated for each cruise, and the heat budget was evaluated for the Gulf of Alaska box. Geostrophic flow was initially selected to be zero at 1500 dbar at all locations around the box. With this choice reference velocity, there was a substantial inflow of mass into the INPOC box with the four-cruise average value of 7 Sverdrups (Sv $\equiv 10^6$ m^3 s^{-1}) and a maximum of 15 Sv in spring 1992. To estimate ''reasonable'' mass inflow into the box, we used the variability of the sea level height in the Gulf of Alaska during the 1997/98 El Niño. As shown in Tropical Ocean Experiment data from the National Oceanic and Atmospheric Adminis-

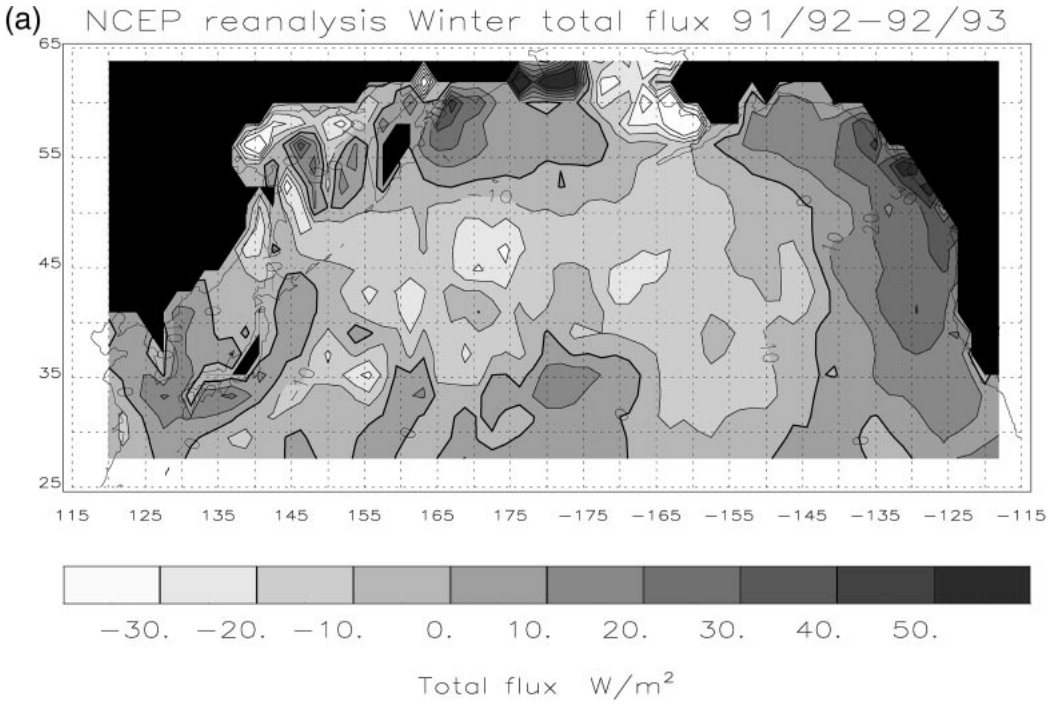

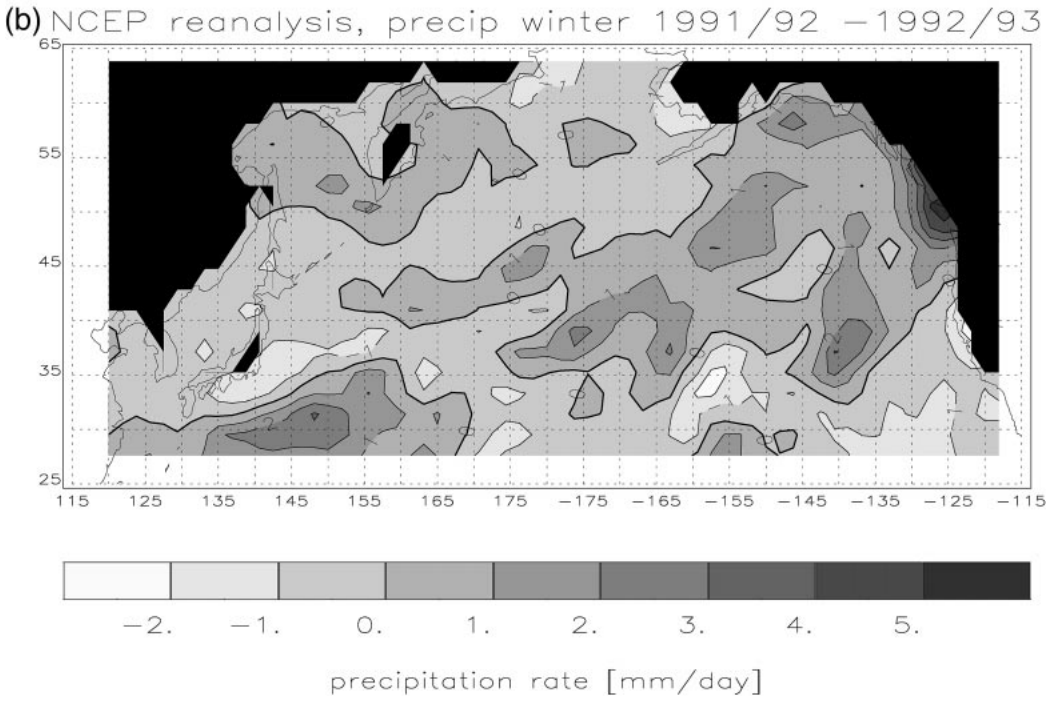

FIG. 4. Differences between the winter of 1991/92 and 1992/93: (a) net surface flux into the ocean and (b) precipitation (from NCEP–NCAR reanalysis).

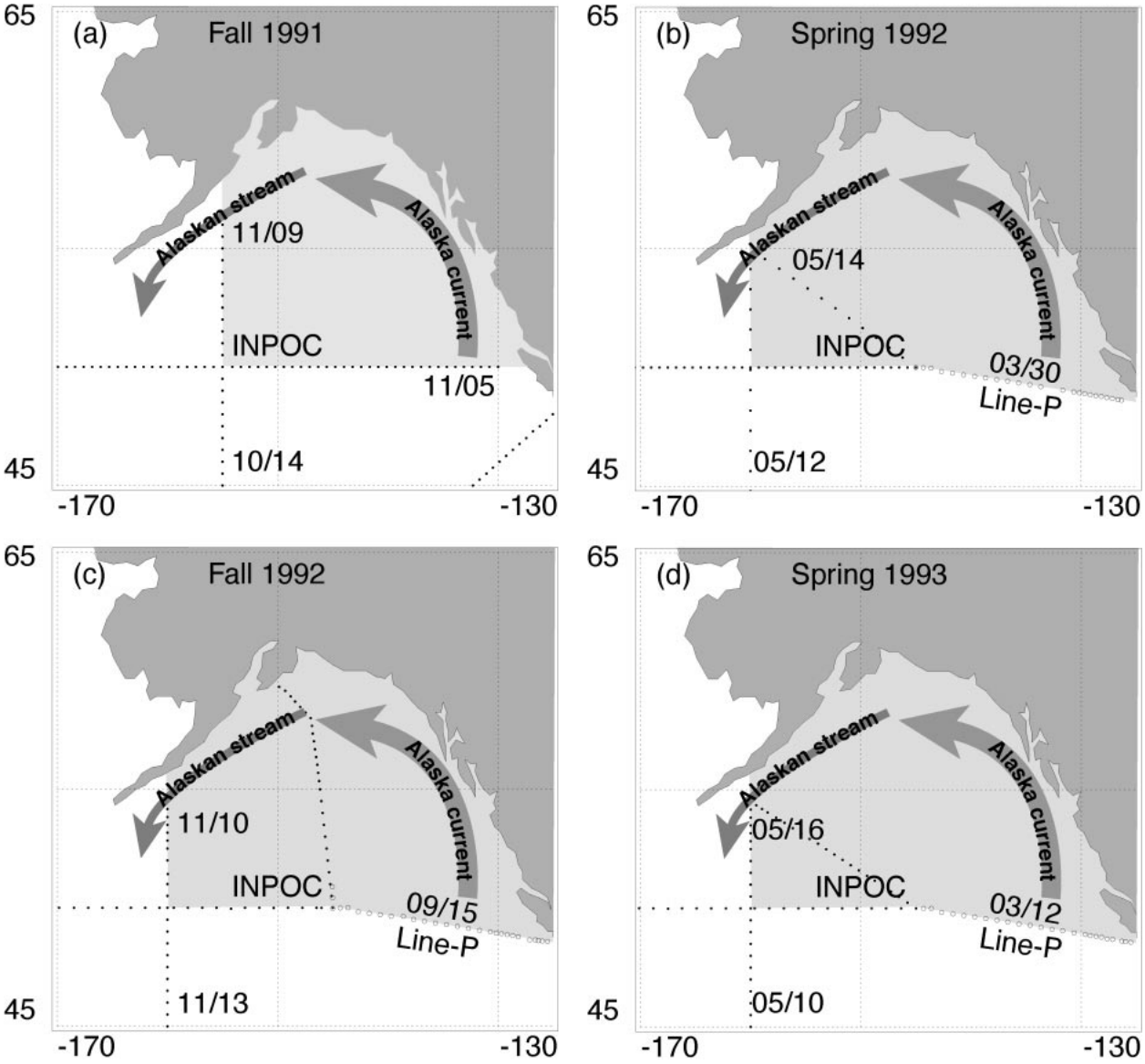

FIG. 5. Station positions in the Gulf of Alaska for the INPOC and Line-P hydrographic cruises: (a) fall 1991, (b) spring 1992, (c) fall 1993, (d) fall 1993. Shading indicates the area of the box used for budget calculations.

tration (NOAA) Laboratory for Satellite Altimetry, the maximum variability is on the 6-month scale with an amplitude of about 10 cm. If we assume that all height changes are due to the mass flux, this value translates into 0.08 Sv mass converegence (or divergence) into the Gulf of Alaska box. Therefore, the net mass flux into the box, including the geostrophic and Ekman flux, must be nearly zero. Because the Alaskan Stream is strong and westward from the surface to the bottom with no zero velocity level, while flow at other locations is much weaker, adjustments to the 1500-dbar velocity for conservation of mass were applied in the Alaskan Stream. The assumed 1500-mb westward flow varied depending on the cruise and on the magnitude of the Ekman divergence used in balancing the total flow. All corrections to the Alaskan Stream were westward and used the average Ekman flow over 3 yr (1991–93) or seasonal averages for each of the four cruises, as described in the next paragraph. The largest velocity used was -8 cm s^{-1} for the spring 1992 cruise. Other adjustments to the geostrophic velocity were also considered, including use of approximate velocities from Reid (1998), or using the various velocity profiles while keeping the mass transport constant. Even though the choice of 1500-db velocity influenced heat transports, our basic results remained unchanged (Table 3).

The Ekman flow was calculated from monthly averaged European Centre for Medium-Range Weather Forecasts (ECMWF) wind stress analyses. The Ekman mass divergence out of the box, averaged over the 3 yr

TABLE 1. Geostrophic volume transport (in Sverdrups) from the INPOC/Line-P box in the Gulf of Alaska. Tr50 indicates meridional transport between the shore and 160°W, with positive being northward, calculated from the 50°N transect. Tr160 is the zonal transport from the 160°W transect, with positive being eastward.

Cruise	Tr50	Tr160	Net (balanced by mean Ekman)
Fall 1991	6.4	−5.1	1.3
Spring 1992	15.5	−14.4	1.3
Fall 1992	10.6	−9.3	1.3
Spring 1993	11.0	−9.7	1.3

TABLE 3. Area-averaged surface heat fluxes (W m^{-2}) from the ocean to the atmosphere in the Gulf of Alaska, calculated from the heat transported into the region by geostrophic and Ekman flow. In A, the geostrophic transport is adjusted to balance the Ekman transport into the box averaged over period 1991–93. In B, mass is balanced using the Ekman transport from the 3-month average for the period of each cruise (3.4 Sv for fall 1991, 0.78 Sv for spring 1992, −5.5 Sv for fall 1992, and −0.3 Sv for spring 1993).

	Balance A		Balance B	
Cruise	Geostrophic	Ekman	Geostrophic	Ekman
Fall 1991	30	−17.0	47	−61.0
Spring 1992	74	−17.0	60	10.0
Fall 1992	18	−17.0	44	−85.0
Spring 1993	36	−17.0	30	2.0

including the cruises (1991–93), was 1.3 Sv. The Ekman mass divergence exhibited strong seasonal variability, with the maximum in late fall and winter and minimum in late spring and summer. When averaged over the time of each INPOC cruise—that is, from March to May for spring, and from September to November for fall—the Ekman divergence was −3.4 Sv for fall 1991, 0.78 Sv for spring 1992, −5.5 Sv for fall 1992, and −0.3 Sv for spring 1993. For heat and mass transports in the Gulf of Alaska both of these approaches were used (the 3-yr average of 1.3 Sv, which we denote balance A, and the 3-month averages for each cruise, which we denote balance B). For Ekman heat transports, potential temperature averaged over the top 100 m was used, based on the cruise data.

The resulting mass and heat fluxes are shown in Tables 1, 2, and 3.

Two realizations of each season do not provide enough information for conclusive results about seasonal and interannual variability. However, we see a tendency for the fall meridional transports across 50°N to be lower than in the spring—this is due to the southward flow at the eastern boundary in each of the two fall cruises, which might result from northward migration of the subtropical gyre through the summer. This corresponds to seasonal changes in the atmospheric forcing, as the Aleutian low is farther south in winter–spring than in summer–fall. Otherwise seasonality in the Alaska gyre is expected to be small (Musgrave et al. 1992).

Maximum heat transport is found in spring 1992, associated with maximum mass transports across 50°N and 160°W. This cruise followed the winter with largest tropical SST anomalies and lowest pressures in the Aleutian low. Thus the larger transport in 1992 compared with 1993 could be an interannual response. For example, Chelton and Davis (1982) show that during El Niño years more water flows into the Alaska Current since the Aleutian low is stronger, while during La Niña, subpolar waters can be found in the subtropical gyre along the California coast.

For all four cruises (Table 3), the geostrophic circulation tends to bring heat into the Gulf of Alaska, especially in the spring. This heating is partially offset by the Ekman circulation, which is dominated by southward transport across 50°N driven by the westerlies, and which removes heat from the region. The cooling related to Ekman flow is largest in late fall and winter when the surface wind stress is the strongest, and close to zero or slightly positive in late spring and summer. When averaged over 3 yr (1991–93), Ekman flow removes the equivalent of about 17 W m^{-2} from the Alaskan box. The individual Ekman transport influenced to some extent the results for the heat convergence calculations. Since the average Ekman flow in both springs (balance B) was lower then for the 3-yr average (balance A), the westward velocity along 160°E had to be increased to balance the mass inflow along 50°N. Therefore the heat convergence by the geostrophic flow decreased. This decrease was to some extent balanced by heat transport by the Ekman flow. The opposite was true for the fall cruises, which were characterized by large Ekman transport related to the strong surface winds. Overall, including the variable Ekman transport deepened the seasonal vari-

TABLE 2. Advective heat transports in the Gulf of Alaska, by the geostrophic flow (W). Tr50 indicates meridional heat transport relative to 0°C calculated from the 50°N transect, with positive northward. Tr160 is the zonal heat transport across the 160°W transect, with positive eastward. The net is the total geostrophic heat transport into the box with the positive sign indicating heating by circulation. The net heat flux is the net heat transport divided by the surface area inside the box (1.8×10^{12} m^2 for the fall 1991 cruise and 1.8×10^{12} m^2 for other cruises) and represents the net heat that must be exchanged between the ocean and the atmosphere; positive indicates that the ocean loses heat to the atmosphere.

Cruise	Tr50 heat transport	Tr160 heat transport	Net transport	Net heat flux
Fall 1991	12.9×10^{13}	-7.2×10^{13}	5.4×10^{13}	30.0
Spring 1992	33.5×10^{13}	-17.7×10^{13}	15.5×10^{13}	74.0
Fall 1992	21.0×10^{13}	-17.1×10^{13}	3.8×10^{13}	−23.0
Spring 1993	21.5×10^{13}	-13.8×10^{13}	7.7×10^{13}	−9.0

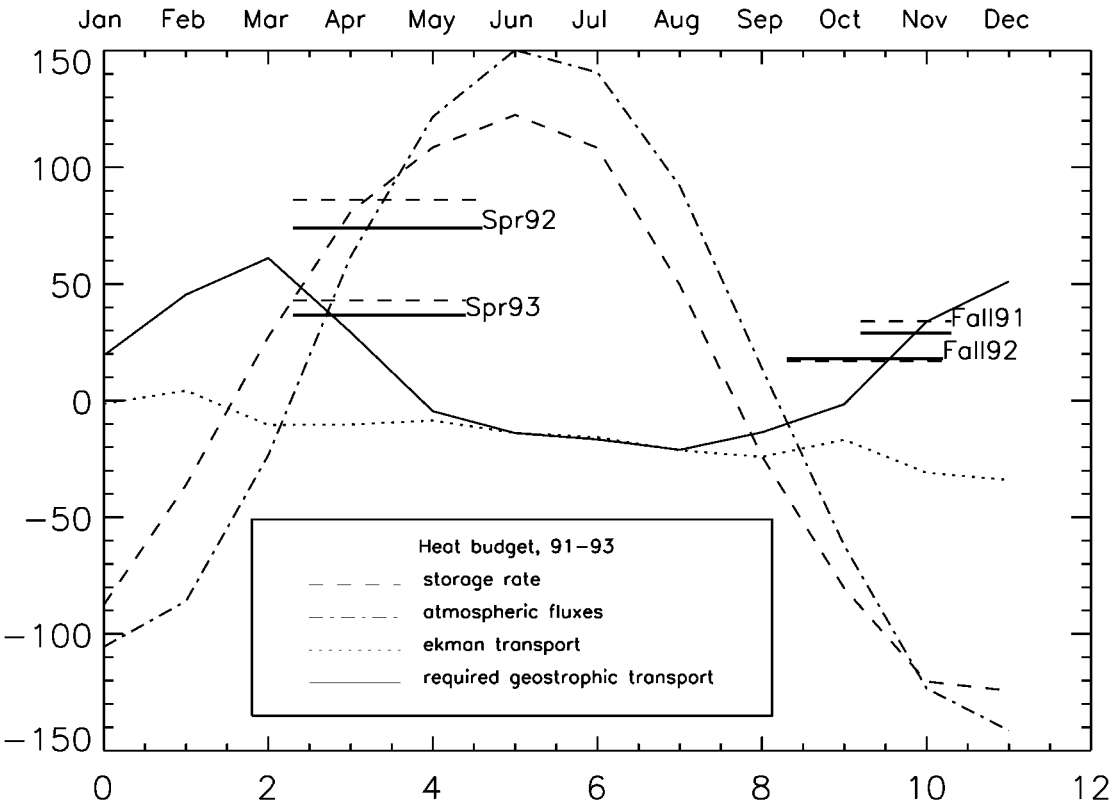

FIG. 6. Heat storage budget (in W m^{-2}), in the Gulf of Alaska averaged over 1991–93. Dashed line: heat storage rate from 0 to 400 db from XBTs from JEDA. Dot–dashed: total flux of heat from the atmosphere to the ocean from the NCEP–NCAR reanalysis. Dotted: heat flux associated with the Ekman circulation calculated from ECMWF wind stress data and monthly climatological temperatures from Levitus and Boyer (1994); positive indicates that heat is brought into the region. Solid: residual flux by geostrophic circulation required to close the budget; positive indicates that heat is brought into the region. The thick lines show the advective, geostrophic heat flux calculated for the INPOC cruises assuming the same average Ekman flux applied to each cruise (balance A), with solid lines indicating transport in the upper 1500-db layer and dashed lines indicating transport in the upper 400-dbar layer.

ability in the oceanic heat transport, while the difference between spring 1992 and 1993 remained the same.

We next examine the full seasonal cycle of heat in the Gulf of Alaska (Fig. 6) using air–sea fluxes from the NCEP–NCAR reanalysis (H_{atm}), heat storage for the 0–400-m layer from the JEDA gridded products based on XBTs (H_{stor}), and Ekman transports across the box boundaries calculated from the ECMWF winds (H_{ek}). The residual of these quantities,

$$H_g = H_{\text{stor}} - H_{\text{atm}} - H_{\text{ek}},$$

is the heat transported into the box by the geostrophic circulation, which is the solid curve in Fig. 6. Warming within the box by the ocean's geostrophic transport should be largest in the spring, roughly at the time of the INPOC spring cruises, while slight cooling is required in summer.

For the period of 1991–93 shown in Fig. 6, the average heat storage rate based on XBTs from JEDA is 2 W m^{-2}, and the average heat flux from the atmosphere to the ocean is 3.2 W m^{-2}, which gives -1 W m^{-2} of required residual cooling by ocean processes. This very small amount is much less than the usual error estimate of several tens of Watts per square meter. (Trenberth 1997) for surface heat fluxes and so is not significantly different from zero. However, the average Ekman heat transport is -17 W m^{-2} (Table 3), which is significant, and so the average annual heating of the Gulf of Alaska by the geostrophic transport must also be significant (16 W m^{-2}) and nearly offsets the Ekman cooling.

The heat fluxes associated with the geostrophic transport calculated directly from the INPOC data and average Ekman fluxes are also shown in Fig. 6. They fit reasonably well on the geostrophic transport curve, particularly for the fall. The spring cruise estimates suggest that the residual curve is biased low.

The total (geostrophic + Ekman) oceanic heat advection averaged over all INPOC cruises indicates a total warming of 22 W m^{-2} for balance A (1991–93 average Ekman flow) and of 11 W m^{-2} for balance B (cruise-dependent Ekman flow). However, the geostrophic transport curve in Fig. 6 shows that both the fall and spring cruises occurred when the Gulf of Alaska

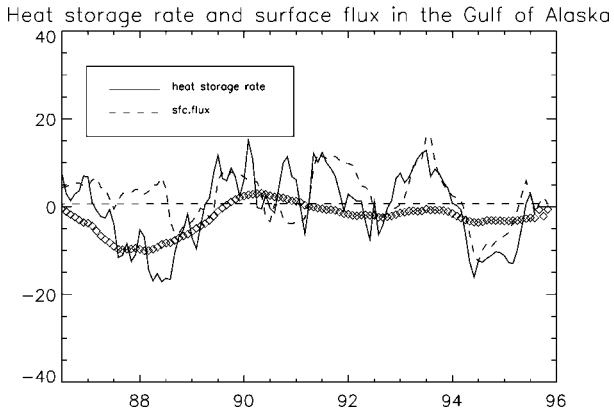

FIG. 7. Twelve-month running average of heat storage rate and atmospheric flux (W m^{-2}) from 1986 to 1995. The circles denote residual ocean transport (24-month running average).

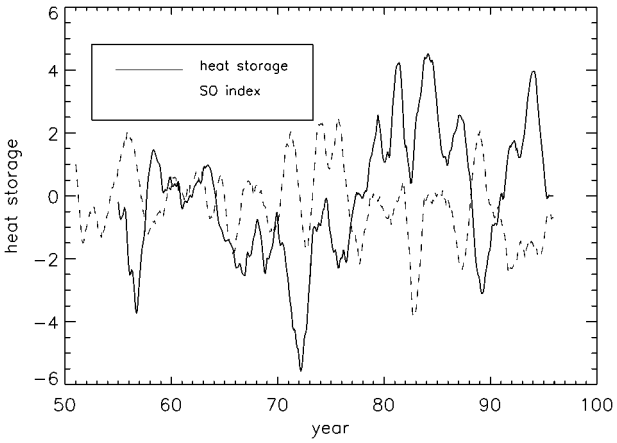

FIG. 8. Twelve-month running average of heat storage anomaly from JEDA and SOI from 1955 to 1996.

should be warming by geostrophic transport, whereas in summertime the opposite is the case.

Our small positive net gain of heat by the ocean from the atmosphere in the Gulf of Alaska is determined by the NCEP–NCAR air–sea fluxes, whose annual average of 3.2 W m^{-2} is not significantly different from zero. A new heat budget for the North Pacific (Moisan and Niiler 1998), on the other hand, shows much larger heat gain by the ocean from the atmosphere in the Gulf of Alaska, on the order of 20–30 W m^{-2}. If we had used these fluxes along with the JEDA heat storage rates and the Ekman heat transport out of the region, then our geostrophic circulation would have been required to cool rather than warm the Gulf of Alaska. All four of our cruises indicate warming by the geostrophic flow, consistent with northward inflow of warm waters across 50°N and outflow of colder waters westward in the Alaskan Stream across 160°W. The consistency of our heat transports calculated directly from the geostrophic velocities with those calculated as residuals suggests that the Moisan and Niiler (1998) heat fluxes may be too high. It is possible that narrow boundary regions of large heat loss were not captured by the coarse spacing of their calculation (P. Niiler 1998, personal communication).

An idea of the role of ocean transport in the Gulf of Alaska heat budget during warm and cold episodes in the Tropics can be made from the surface heat budget for the last 10 yr, covering the 1988/89 La Niña and the 1991–94 El Niño. We used monthly surface fluxes from the NCEP–NCAR reanalysis and gridded storage anomalies from JEDA (White 1995) to find the required ''residual'' ocean transport. The results of this calculation are shown in Fig. 7. The atmospheric fluxes are, on the average, larger than zero, meaning heating of the ocean by atmosphere. The heating increases slightly during El Niño. The ocean storage rate variability has greater magnitude, with values roughly close to atmospheric fluxes during El Niño but significantly smaller during La Niña in late 1980s. This results in negative ocean heat transport during La Niña and close to zero transport in El Niño years. The calculation presented here is subject to large errors, since the small net terms result from differences in relatively large fluxes. However, the comparison of the heat storage in the Gulf of Alaska with the SOI indicates that positive heat storage anomaly is usually associated with negative SOI (El Niño), while a negative anomaly corresponds to La Niña (Fig. 8). The increase in heat storage during El Niño years, not entirely compensated by atmospheric fluxes, qualitatively agrees with our measurements of larger oceanic heat transport during the cruise that occurred at the height of El Niño (spring 1992).

As shown in Table 2, spring of 1992 (strong El Niño) was characterized by large advective geostrophic heat flux into the Gulf of Alaska, associated with the increased strength of the cyclonic circulation. In 1992, the geostrophic heat transport of 15.5×10^{13} W (corresponding to 74 W m^{-2}) was twice as large as the heat transport observed during the following spring. Since at this time of year the Ekman transport was fairly small, it did not balance the large heat fluxes associated with geostrophic flow. This over 30 W m^{-2} difference in the ocean heat transport between El Niño (spring 1992) and more normal (spring 1993) conditions was greater than the difference in surface heat flux from winter 1992 to winter 1993 calculated from the NCEP–NCAR reanalysis (Fig. 4). Therefore it appears that ocean transport is important in creating the SST and heat storage anomalies in the Alaskan gyre.

4. Summary and conclusions

We examined the circulation in the Gulf of Alaska using data from four INPOC hydrographic cruises conducted in the North Pacific from 1991 to 1993, augmented by Canadian Line-P cruises. The fluctuations of the 1991/92 El Niño episode, with maximum tropical anomalies in winter 1991/92 and receding of anomalous

conditions the next winter, presented an opportunity to examine the subpolar North Pacific mass and heat transport during changing tropical conditions.

Because the difference in tropical conditions was more pronounced during and right before spring cruises, the spring 1992 and 1993 cruises were expected to be more useful in estimating the interannual changes of mass and heat transport than the fall 1991 and 1992 measurements. We have shown that following the warm episode in the Tropics at the beginning of 1992, circulation in the Gulf of Alaska was stronger, and the heat transport into the Gulf caused by geostrophic ocean transport was larger than in the following spring. In 1993, after the El Niño weakened in the Tropics, the spring heat transport was over two times smaller—that is, decreased from 70 to 34 W m^{-2}. This heat flux variability is comparable to changes in the net atmospheric surface heat flux and therefore may contribute substantially to temperature anomalies.

We cannot be certain that the difference between Gulf of Alaska circulation in the springs of 1992 and 1993 resulted entirely from the change in atmospheric wind forcing. The atmosphere–ocean system in the North Pacific is subject to interdecadal as well as ENSO-scale changes, and with only 2 yr of data we cannot determine to what extent 1992–93 differences in ocean transport were due to changes in atmospheric forcing related to tropical SST anomalies. The phase of the interdecadal oscillation is at this moment difficult to determine. Even though the pressure in the North Pacific began to rise in the late 1980s (Fig. 2), the warming in the early 1990s caused the NP index to drop again. As shown by Trenberth and Hoar (1996) the 1990–95 period was rather unusual and difficult to fit into a natural oscillation pattern. Nevertheless, the INPOC observations provided the opportunity to compare the heat balance in the Gulf of Alaska for atmospheric circulations in the midlatitudes corresponding to varying SST distributions in the Tropics.

Recent analysis indicates that tropical SSTs can have stronger influence on midlatitude anomalies than previously suggested by global circulation models. Hoerling and Kumar (1997) show that during the 1982/83 ENSO the response to tropical SST anomalies was a major factor determining midlatitude anomalies; the weak midlatitude response to a strong tropical SST forcing that was observed in the Atmospheric Model Intercomparison Project simulations resulted from data assimilation problems. Therefore observations tying the North Pacific Ocean circulation changes to interannual change in the tropical conditions can be of particular interest for the modeling community.

Acknowledgments. This research was supported by NSF Grants ATM 9613772 and OCE92-03880 and by a NOAA Postdoctoral Program in Climate and Global Change fellowship, administered by the University Corporation for Atmospheric Research. We gratefully acknowledge the work of O. Pyatin and G. Yurasov as chief scientists on the *Priliv* cruises, of the scientists and technicians on those cruises, and of F. Whitney and E. Carmack at the Institute of Ocean Sciences, in producing the INPOC and Line-P CTD datasets used herein.

REFERENCES

Alexander, M. A., 1992: Midlatitude atmosphere–ocean interaction during El Niño. Part I: The North Pacific Ocean. *J. Climate,* **5,** 944–958.

Chelton, D. B., and R. E. Davis, 1982: Monthly mean sea-level variability along the west coast of North America. *J. Phys. Oceanogr.,* **12,** 757–784.

Goddard, L., and N. Graham, 1997: El Niño in the 1990s. *J. Geophys. Res.,* **102** (C5), 10 423–10 436.

Hoerling, M. P., and M. Ting, 1994: Organization of extratropical transients during El Niño. *J. Climate,* **7,** 745–766.

——, and A. Kumar, 1997: Origins of extreme climate states during the 1982–83 ENSO winter. *J. Climate,* **10,** 2859–2870.

Horel, J., and J. M. Wallace, 1981: Planetary scale phenomena associated with the Southern Oscillation. *Mon. Wea. Rev.,* **109,** 813–826.

Kalnay, E., and Coauthors, 1996: The NCEP/NCAR 40-Year Reanalysis Project. *Bull. Amer. Meteor. Soc.,* **77,** 437–471.

Lagerloef, G. S. E., 1995: Interdecadal variations in the Alaska gyre. *J. Phys. Oceanogr.,* **25,** 2242–2258.

Latif, M., 1998: Dynamics of interdecadal variability in coupled ocean–atmosphere models. *J. Climate,* **11,** 602–624.

——, and T. Barnett, 1994: Causes of decadal climate variability over the North Pacific and North America. *Science,* **266,** 634–637.

Lau, N. C., and M. J. Nath, 1996: The role of the atmospheric bridge in linking tropical pacific ENSO events to extratropical SST anomalies. *J. Climate,* **9,** 2036–2057.

Levitus, S., and T. Boyer, 1994: *Temperature.* Vol. 4, *World Ocean Atlas 1994,* NOAA, NOAA Atlas NESDIS 4, 117 pp.

McPhaden, M., 1993: TOGA–TAO and the 1991–93 El Niño–Southern Oscillation event. *Oceanography,* **6,** 36–44.

Meyers, S., M. Johnson, M. Liu, J. O'Brien, and J. Spiesberger, 1996: Interdecadal variability in a numerical model of the northeast Pacific Ocean: 1970–89. *J. Phys. Oceanogr.,* **26,** 2635–2652.

Moisan, J. R., and P. P. Niiler, 1998: The seasonal heat budget of the North Pacific: Net heat flux and heat storage rates (1950–1990). *J. Phys. Oceanogr.,* **28,** 401–421.

Musgrave, D., T. Weingartner, and T. Royer, 1992: Circulation and hydrography in the northwestern Gulf of Alaska. *Deep-Sea Res., Oceanogr. Res. Pap.,* **39** (9A), 1499–1519.

Reid, J. L., 1998: On the total geostrophic circulation of the Pacific Ocean: Flow patterns, tracers and transports. *Progress in Oceanography,* Vol. 39, Pergamon, 263–352.

Reynolds, R. W., 1988: A real-time global sea surface temperature analysis. *J. Climate,* **1,** 75–86.

Tabata, S., 1991: Annual and interannual variability of baroclinic transports across Line Pin the northeast Pacific Ocean. *Deep-Sea Res., Oceanogr. Res. Pap.,* **38** (1A) (Suppl.), 5221–5245.

Talley, L. D., 1984: Meridional heat transport in the Pacific Ocean. *J. Phys. Oceanogr.,* **14,** 231–241.

Trenberth, K. E., 1997: Using atmospheric budgets as a constraint on surface fluxes. *J. Climate,* **10,** 2796–2809.

——, and J. W. Hurrel, 1994: Decadal atmosphere–ocean variations in the Pacific. *Climate Dyn.,* **9,** 303–319.

——, and T. Hoar, 1996: The 1990–1995 El Niño–Southern Oscillation event: Longest on record. *Geophys. Res. Lett.,* **23** (1), 57–60.

White, W., 1994: Slow El Niño–Southern Oscillation boundary waves. *J. Geophys. Res.,* **99** (C11), 22 737–22 751.

——, 1995: Design of a global observing system for gyre-scale upper ocean temperature. *Progress in Oceanography,* Vol. 36, Pergamon Press, 169–217.

Zhang, Y., J. Wallace, and D. Battisti, 1997: ENSO-like interdecadal variability: 1900–93. *J. Climate,* **10,** 1004–1020.